

**UC Davis**  
**IDAV Publications**

**Title**

Evaluation of a Human Vision System based Image Fidelity Metric for Image Compression

**Permalink**

<https://escholarship.org/uc/item/70q0r049>

**Authors**

Avadhanam, Niranjana  
Algazi, Ralph

**Publication Date**

1999

Peer reviewed

# Evaluation of a Human Vision System based Image Fidelity Metric for Image Compression

Niranjan Avadhanam\*, V. Ralph Algazi

CIPIC, Center for Image Processing and Integrated Computing,

University of California, Davis, CA 95616

{avadhana\*,algazi}@ece.ucdavis.edu

## ABSTRACT

Conventional mean squared error based methods for objective image quality assessment are not well correlated with human evaluation. The design of better objective measures of quality has attracted a lot of attention and several image quality metrics based explicitly on the properties of the Human Visual System (HVS) have been proposed in recent years. However, only in a few cases has the performance of such metrics been demonstrated on real images. In accounting for visual masking, all these metrics assume that the multiple channels mediating visual perception are independent of each other. Recent neuroscience findings and psychophysical experiments have established that there is interaction across the channels and that such interactions are important for visual masking. In this work, we propose the Picture Distortion Metric (PDM) which integrates these new visual masking properties, and we evaluate its performance for image coding applications. We evaluate the performance at medium to high range of quality to predict subjective scores on a 0-10 numerical scale, and on a wide range of quality for the 1-5 CCIR impairment scale.

**Keywords :** image quality, image compression, psychophysics, human observer, quality assessment.

## 1. INTRODUCTION

Conventional mean squared error based methods for objective image quality assessment are not well correlated with human evaluation.<sup>1,2</sup> The design of better objective measures of quality have attracted a lot of attention in the past two decades.<sup>3-10,2</sup> Ahumada<sup>11</sup> gave an overview of quality metrics for image degradation which includes methods for half-toning, image compression and image processing. More recently, Eckert *et al.*<sup>12</sup> gave a review of perceptual quality metrics and a discussion of various components of typical objective quality metrics, for still image compression applications.

In general, objective measures quantify one or more distortion factors defined as distance measures on perceptually transformed original and degraded images. These metrics compute the distance measure on the outputs of a multi stage model; each stage accounting for properties of visual perception relevant to the visibility of distortions. In recent years several image quality metrics based explicitly on the properties of the HVS have been proposed.<sup>13,5,14,15,7,10,6</sup> These metrics compute a distance measure based on the outputs of a multiple channel cortical model of human vision which accounts for known sensitivity variations of the HVS in the primary visual pathway. The promise of a metric based on the HVS is that it would be very general in its nature and applicability. In addition to correctly describing threshold behavior, if it could accurately rate supra-threshold errors, it can be used to evaluate any image processing algorithm, regardless of the types of distortions it introduces.

Metrics based on HVS models have been developed based on psychophysical threshold-based experiments which predominantly measure responses to simple stimuli like gratings or gabor patches. It is very important to verify the performance of such metrics on complex supra-threshold stimuli such as natural images, and this has been demonstrated only in a few cases.<sup>15,5,7</sup> The Visible Differences Predictor (VDP)<sup>6</sup>

proposed by Scott Daly and the Lubin model<sup>15</sup> are examples of carefully designed metrics whose performance have been demonstrated on relatively simple psychophysical stimuli as well as complex stimuli like images. All these metrics assume that the multiple channels mediating visual perception are independent of each other. Recent neuroscience findings have shown that there is significant interaction across the channels.<sup>10,16,17</sup> There is also strong evidence from psychophysical experiments that interactions across channels are very important for visual masking.<sup>18,19</sup> In particular, Foley has shown that a new psychophysical masking model incorporating these interactions gives significantly better results than models which assume no interaction.<sup>19</sup> In this work, we propose the Picture Distortion Metric (PDM) which integrates these new visual masking properties, and we evaluate its performance for the important case of still image coding. We first evaluate the performance of the PDM in predicting quality scores from medium to high quality. We then apply the PDM for predicting quality scores which are in a wide range of quality from low to high.

This paper is organized as follows: After a brief introduction in section 1, we present the PDM methodology in section 2. That section gives a brief description of all the components of the PDM. In section 3, we present results evaluating the performance of the PDM at medium to high range of quality to predict subjective scores on a new 0-10 numerical scale, and on a wide range of quality for the 1-5 CCIR impairment scale. Finally, in section 4, we present a discussion of the metric and its performance and some conclusions.

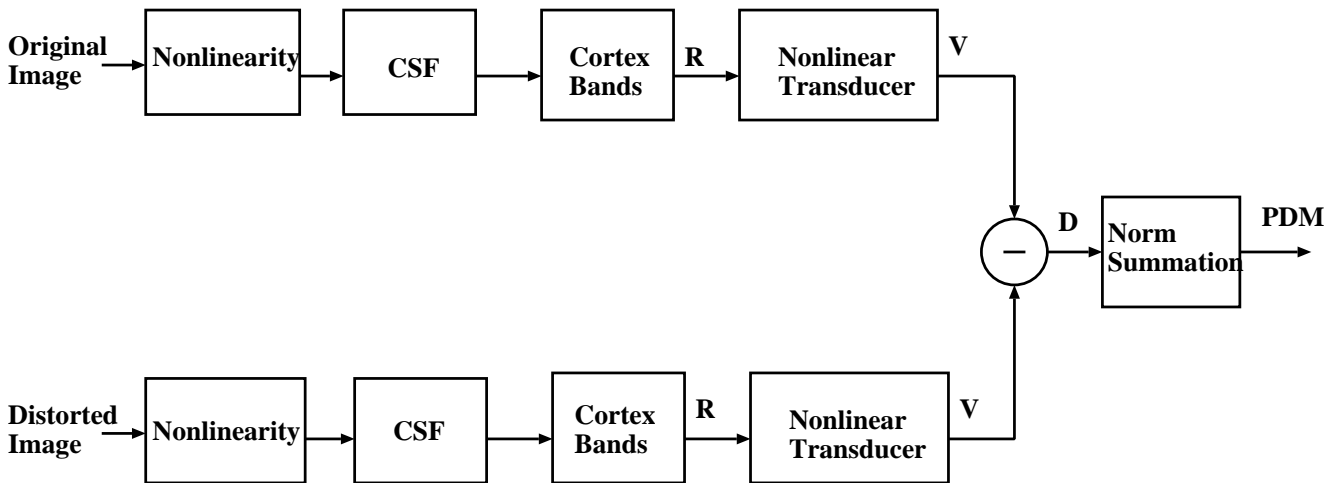


Figure 1. Picture distortion metric

## 2. METHODOLOGY

Objective metrics used for quality evaluation of coded images should approximate closely the visual quality assessment by the human observer. For a coded image, the stimulus assessed by the observer is the coder error and the masking pattern is now the local activity in the image which may reduce the visibility of the error. The visibility of the errors is also affected by the background luminance level, and by the spatial structure and the frequency content of errors. Using the properties of vision, the goal is to quantify these coder errors by a measure that reflects their visibilities.

In figure 1 we show a diagram of the PDM model. The main components of the model are:

1. perceptual nonlinearity

2. contrast sensitivity function
3. orientation and frequency selective bands (cortex bands)
4. visual masking properties, denoted “nonlinear transducer”.
5. error summation.

### 2.1. Perceptual nonlinearity

Note that a display nonlinearity may be needed to generate luminances corresponding to image gray values. We then use a simple power law on the luminances to model the input perceptual nonlinearity which maps physical luminances to perceptual brightness. This results in a brightness image  $b(x, y)$ .

### 2.2. Contrast sensitivity function

We adopt the CSF and the orientation and frequency selective decomposition from the VDP.<sup>6</sup> In general, this CSF is bandpass in shape, reflecting visual perception properties at threshold. A low pass version of this CSF is used in this work as it is regarded to be more appropriate for the supra-threshold conditions seen in image quality rating applications.

### 2.3. Orientation and frequency selective decomposition

The orientation and frequency selective decomposition is adopted from the VDP<sup>6</sup> and uses 5 frequencies and six orientations so that there are 31 cortex bands when the isotropic low pass baseband is included. The orientation bandwidth is 30 degrees and the frequency bandwidth is 1 octave for each cortex band. The decomposition results in 31 brightness images  $b_{k,l}(x, y)$ , corresponding to each cortex band, where  $k, l$  correspond to the indices of frequency and orientation selective channels. To compute the contrast in each cortex band, we use the simple definition of global contrast and normalize by the image mean. That is, we obtain 31 contrast images  $c_{k,l}(x, y)$  where

$$c_{k,l}(x, y) = \frac{b_{k,l}(x, y)}{b_{mean}} \quad (1)$$

Note that we use analytic filters so that 31 image sets exist corresponding to both odd and even symmetric simple cell responses.

### 2.4. Visual masking

Typically, visual masking is incorporated by using threshold elevation or a saturating transducer function. When a transducer function is used, the output of the cortex filters are assumed to be the components of a multidimensional feature vector. The coding errors are quantified by the  $L_p$  norm of the difference between the masker (original image) and the masker + stimulus (coded image). The final metric is hence the distance between the vectors representing the original image and the coded image.

#### 2.4.1. New approach to masking

Previous HVS metrics assume that the cortex bands representing the multiple channels in the HVS are independent of each other. It has been shown by recent results in neuroscience and psychophysics studies<sup>10,20,18</sup> that there is significant interaction between different cortex bands. The performance of a HVS metric may be expected to improve if we take this into consideration.<sup>10</sup> The generalized normalization model proposed by Watson *et al.*<sup>21,22,18</sup> will be able to account for interactions between cortex bands

as reflected in masking. The responses from the frequency and orientation selective cortex bands are transformed into normalized responses as

$$V = \frac{aR_{exc}^p}{b + \sum_{\Omega} R_{inh}^q} \quad (2)$$

where  $R_{exc}$  and  $R_{inh}$  are the response of neurons in the excitory and inhibitory paths and  $V$  is the normalized response.<sup>21,22,18</sup> Both odd and even symmetric simple cell responses are considered for the excitory and inhibitory paths. Separate excitory paths for even and odd symmetric simple cell responses are used whereas the inhibition is common to both paths and uses energy summation over even and odd symmetric responses. Note that the pooling operation given by  $\sum_{\Omega} R_{inh}^q$  can be over orientation, frequency and spatial extent. This extent accounts for the spread of masking among different neural layers. In this work, only orientation pooling between bands at the same spatial frequency is implemented. At this point, it should be noted that there are several types of masking,<sup>23</sup> some of which cannot be easily modeled. We have considered only pattern masking<sup>18</sup> in this work. In other words, the model assumes that the mask is a simple deterministic pattern, for example, a gabor patch.

We compare this masking to the within channel transducer masking proposed by Legge and Foley<sup>24</sup> which uses

$$V = \frac{a|R_{exc}|^{2.4}}{b + |R_{inh}|^2} \quad (3)$$

A similar model was used in Lubin's work.<sup>14,15</sup>

Using the notation of equation 1, the normalized responses for each band are calculated as

$$V_{k,l}(x, y) = \frac{a(c_{k,l}(x, y))^p}{b + \sum_{\Omega} (c_{k,l}(x, y))^q} \quad (4)$$

## 2.5. Summation of partial responses

For overall summation over all frequency and orientation selective bands and spatial locations, we have experimented with summations of norms 2, 4 and 8. The overall metric for a norm 'q' summation over all frequency  $k$  and orientation  $l$  selective bands and norm 'p' over all spatial locations  $(x, y)$  is computed as

$$PDM = \left( \sum_{X,Y} PDM(x, y)^p \right)^{\frac{1}{p}} \quad (5)$$

where

$$PDM(x, y) = \left( \sum_{K,L} D_{k,l}(x, y)^q \right)^{\frac{1}{q}} \quad (6)$$

and

$$D_{k,l}(x, y) = V_{k,l,o}(x, y) - V_{k,l,c}(x, y) \quad (7)$$

here, the subscripts  $o$  and  $c$  correspond to the original and compressed images.

We evaluated the three summations, the first being a norm2 over all bands and spatial locations. This reflects energy summation. The second one is a norm4 summation over all bands and spatial locations and approximates probability summation.<sup>25</sup> Thirdly, we use a norm4 summation over all bands to approximate probability summation over multiple channels and then a norm8 summation over all spatial locations (which gives preference to larger errors) to compute the global metric. All the reported results are for this two step summation. If desired, the PDM output before the summation over spatial locations, can be used as a distortion map. These maps can be used to gain useful insight into the performance of the coder in

different parts of the image. For this paper, however, we use the summed scalar metric as an indicator of the overall quality of the image. It should be noted here, that it is not clear what is the correct way to sum over all the bands and especially all the spatial locations.<sup>12</sup> Hence, we use a simple norm summation for the PDM computation. Better methods of summation may yield improved results; especially if results from the study of higher order perceptual properties like eye movements are also incorporated.

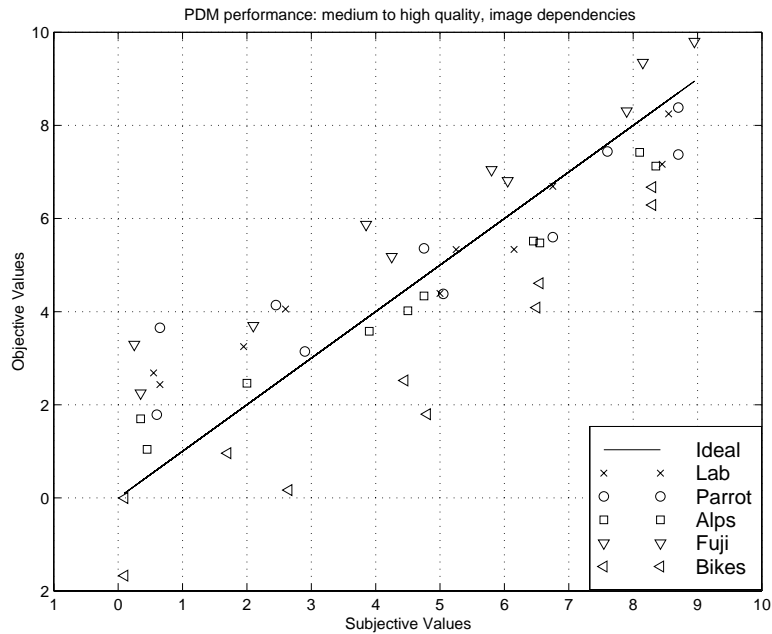


**Figure 2.** Picture distortion metric at higher quality ranges: image dependencies

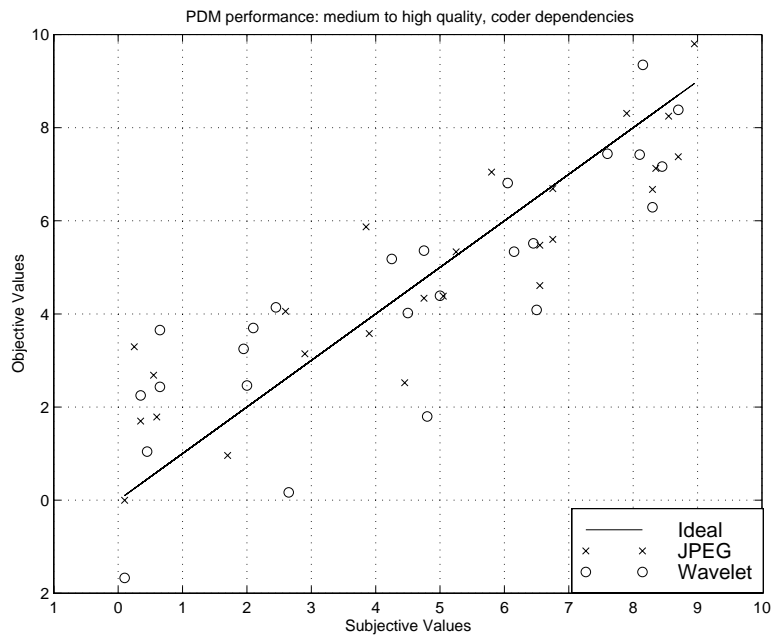


**Figure 3.** Picture distortion metric at higher quality ranges: coder dependencies

### 3. RESULTS

We now demonstrate the performance of the PDM in predicting subjective scores for coded images. The raw PDM output values are linearly transformed (in the least square error sense) to obtain a final PDM metric which can be directly compared with subjective scores. It is important to note that this does not change the correlation coefficient and the rank correlation values, but all other observations (image and coder dependencies) are based on this linearly transformed metric.



**Figure 4.** Test images 1: top: Lab, Parrot, Alps; bottom: Fuji, Bikes.

#### 3.1. High Quality Results

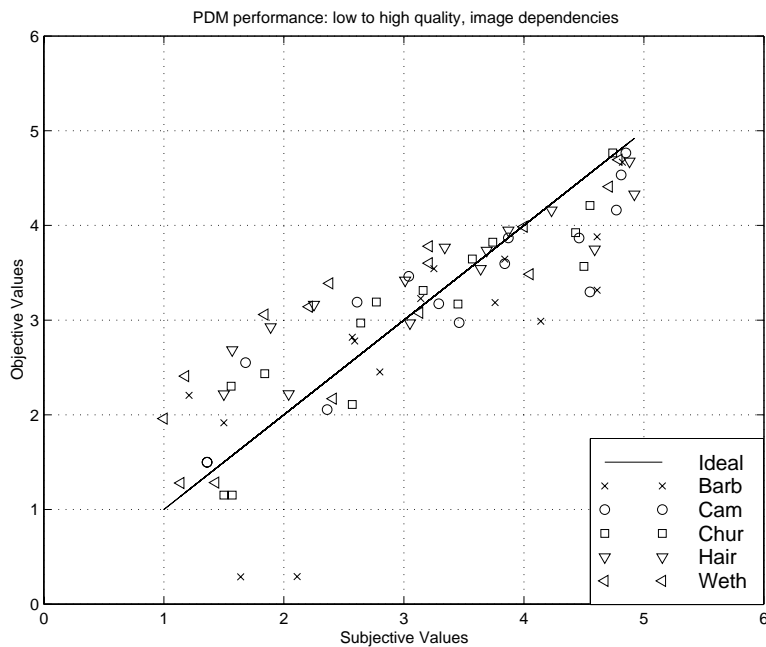
We first evaluate the performance of the PDM for medium to high quality range images. The subjective scores were obtained using a 3-context image assessment scheme for coded images.<sup>26,27</sup> In this method, separate scales are obtained for images differing in scene content and for each coding algorithm, using numerical category scaling with explicit high and low anchors. Since images obtained at different quality levels from each scene and coder are separately rated, we avoid the problems of numerical scaling wherein subjects use separate scales to rate distinct images and coders. Further, the method uses explicit anchor stimuli specifying the end points of the scale. By presenting unambiguous anchors specifying the ends of the scale each time an image is rated, this method assures dependable results. The separate scales are linked using pairwise matching techniques to obtain a robust scaling technique. This method can be used for arbitrary, narrow ranges of quality.

Figure 4 shows the five 512\*512 sized test images (denoted "Bikes", "Lab", "Alps", "Fuji" and "Parrot") which were selected from a Kodak PhotoCD disc. Two coders were selected for the experiments: the standard JPEG coder<sup>28</sup> (Independent JPEG Group IJPG Version 6) and a wavelet coder<sup>29,30</sup>(biorthogonal, "9-7" wavelet of Barlaud,<sup>31</sup> four dyadic scales, HVS based quantizer and an activity mask based QM

encoder) that produce artifacts of widely varying visual effect. The experiments focused roughly on medium to high quality, with five levels of quality for each image, giving a set of 50 images (5 images\*2 coders\*5 levels/coder). Five observers took part in the experiments; two having extensive experience in viewing coded images, one with moderate experience and the other two having minimal experience. All of them had normal/corrected to normal vision. The individual subjective scores were averaged to obtain a subjective score for each image.

The database consists of 50 images rated on a 0-10 numerical scale over medium to high range of quality. Figure 2 shows the performance of the PDM in predicting subjective scores. The correlation coefficient and the rank correlation between the PDM and subjective scores are 0.87 and 0.89. The performance is good, especially at higher levels of quality. There is an image dependency in the performance (as shown in figure 2), with the metric consistently underestimating subjective scores for the "Bikes" image and consistently overestimating scores for the "Fuji" image. It is interesting that exclusion of the "Bikes" image from the database results in a correlation of 0.93. This is because the "Bikes" image is very busy with a large number of features, yielding larger coding errors. These larger distortions are given more importance by the PDM, whereas the subjects do not, while giving their subjective scores. There is no strong coder dependency of the performance as shown in figure 3. Since the metric is based largely on properties of threshold vision, it is expected to work better at high quality, and we can verify this from figure 2.

We now compare the performance of inter-channel masking used in the PDM with the intra-channel masking used in previous studies,<sup>15</sup> keeping the rest of the model same. The PDM with inter-channel masking performs better, achieving correlation 0.87 and rank correlation 0.89 with subjective scores, as compared to correlation of 0.85 and rank correlation of 0.85 obtained using intra-channel masking. Further, the mean and the maximum of the absolute prediction error using the PDM with inter-channel masking are 1.19 and 3.04, lower than the corresponding values, 1.24 and 3.5 with intra-channel masking. Although this comparison shows that inter-channel masking performs better than intra-channel masking, it should be strongly emphasized that the comparison is strictly within the PDM framework and specifically for the task of predicting subjective quality scores.



**Figure 5.** Picture distortion metric for wide quality range: image dependencies





**Figure 6.** PQS test images. From left to right, then top to bottom: Church, Hairband, Weather, Barbara, and Cameraman.

### 3.2. Wide Quality Range Results

We next evaluate the performance of the metric on a database of images which are in a wide range of quality. The subjective scores were obtained on the CCIR impairment scale.<sup>2</sup> Figure 6 shows the 256\*256 sized test image set which include the ITE (Institute of Television Engineers of Japan) test images “Church”, “Hairband” and “Weather”, and the widely used “Barbara”, and “Cameraman” images. The JPEG coder and simple wavelet and subband coders were used to compress the images.<sup>2</sup> The experiments resulted in a set of five images coded with one of three types of coders and for the entire range of quality. A total of seventy five encoded images were assessed by nine observers as described, and the average MOS score was computed for each encoded image.

The database consists of 75 images obtained by compressing five test images using 3 coders at 5 levels of quality. Figure 5 shows the performance of the PDM in predicting subjective scores. The correlation coefficient and the rank correlation between the PDM and subjective scores are 0.85 and 0.9. The performance is good, especially at higher levels of quality, as discussed before. There is no strong image or coder dependency in the performance. For this quality range, there is a non-linear relationship between the PDM and the subjective scores which can be seen in the figure 5. It is very interesting to see that the measure performs very poorly while predicting the quality of two particular images. These sub-band coded “Barbara” images, have severe Moire pattern-like artifacts in the scarf region. The PDM gives lot of importance to these errors while the subjects do not, when they judge the quality. The discrepancy in such results shows the inherent limitation of present generation HVS based objective quality measures which do not model the higher order visual attention and memory processes which play an important role in subjective image quality judgment.

## 4. DISCUSSION AND CONCLUSIONS

In this paper, we develop a new vision model based objective metric, the PDM, which incorporates new masking models proposed in psychophysics literature.<sup>19,18</sup> In addition, we show that such a distortion metric based largely on threshold properties of the HVS performs well in predicting subjective score values at high quality and reasonably well at lower levels of quality.

However, there are several reasons why vision models should be applied with caution to natural images: vision models have been developed based on psychophysical experiments a vast majority of which involve threshold measurements only; the extension of these models to supra-threshold image error conditions may not be entirely appropriate. In addition to this, most psychophysical experiments measure responses to simple stimuli like gratings or gabor patches. It may not be possible to extend some of these results to analysis of complex stimuli like compressed images. In spite of these limitations, the success of applying properties of visual perception for image processing or coding applications have been reported through the years.<sup>13,32–35</sup>

In this work, we have used the terms image quality and image fidelity quite loosely and occasionally interchangeably. But, strictly, there are significant differences between the two. We now consider the difference between subjective image quality and image fidelity and how they relate to the performance of objective metrics. Image fidelity quantifies how accurately a process, for example, a display, renders an image. The fidelity of the rendered image is how visually discriminable it is, from the original image. The fidelity of the rendered image, can be quantified objectively, for example, by using HVS metrics which can quantify the discriminable differences. Image quality, on the other hand, quantifies how much one image is preferred over the other. There are several additional factors which mediate subjective quality evaluation. These include individual preferences, past memory and expectations of the observer and several cognitive factors which are difficult to even identify. It has been shown that there is a complex relationship between image quality and fidelity, which depends on the specific task.<sup>36</sup> Subjective assessment of images involves both fidelity and quality; the results depend on how the attributes and instructions are described and used while performing the experiments. For all the subjective data used in this paper, subjective evaluation was performed using image impairment (rather than image quality) as an attribute as described in the references.<sup>26,27,2</sup> We have noticed in our work, similar to other studies,<sup>37</sup> that the results of the subjective experiments are dependent on the instructions used. We postulate that when observers scale impairment rather than quality, using anchored scales, the assessment uses a combination of image fidelity and image quality depending on the level of quality. However, this issue was not rigorously explored in our work on subjective quality.<sup>26,27</sup>

HVS based objective metrics are actually, image fidelity metrics. It can be argued that there is a limitation on how well HVS based objective fidelity metrics can predict subjective scores which are a reflection (at least partly) of image quality. The performance of the HVS based objective fidelity metrics in predicting subjective scores is not only limited by the threshold data used to derive the properties of the model, but also by the lack of the cognitive factors that are involved in the subjective assessment. Incorporating some of the higher level visual and cognitive processes would improve the performance of HVS based objective metrics.

## REFERENCES

1. H. Marmolin, "Subjective MSE measures (picture processing)," *IEEE Transactions on System, Man, and Cybernetics*, vol. SMC-16, pp. 486–489, May 1986.
2. M. Miyahara, K. Kotani, and V. Algazi, "Objective Picture Quality Scale (PQS) for image coding," *IEEE Transactions on Communications*, vol. 46, pp. 1215–1226, Sept. 1998.
3. J. L. Mannos and D. J. Sakrison, "The effects of a visual fidelity criterion on the encoding of images," *IEEE Trans. Info. Thy.*, vol. IT-4, no. 4, pp. 525–536, 1974.
4. J. O. Limb, "Distortion criteria of the human viewer," *IEEE Transactions on System, Man, and Cybernetics*, vol. SMC-9, pp. 778–793, Dec. 1979.
5. C. Zetzsche and G. Hauske, "Multiple channel model for the prediction of subjective image quality," in *Proc. SPIE*, vol. 1077, pp. 209–216, SPIE, 1989.
6. S. Daly, "The Visible Difference Predictor: An Algorithm for the Assessment of Image Quality," in *Digital Images and Human Vision* (A. Watson, ed.), Cambridge, Mass.: MIT Press, 1993.

7. S. Westen, R. L. Lagendijk, and J. Biemond, "Perceptual image quality based on a multiple channel HVS model," in *Proceedings, International Conference on Acoustics, Speech, and Signal Processing*, vol. 4 of *ICASSP 95*, pp. 2351–2354, ICASSP, 1995.
8. S.A. Karunasekera and N.G. Kingsbury, "A distortion measure for blocking artifacts in images based on human visual sensitivity," *IEEE Transactions on Image Processing*, vol. 4, pp. 713–724, June 1995.
9. W. Xu and G. Hauske, "Picture quality evaluation based on error segmentation," in *Proceedings of SPIE, Visual Communications and Image Processing*, vol. 2308, pp. 3:1454–65, SPIE, 1994.
10. P. Teo and D. Heeger, "Perceptual image distortion," in *1994 SID International Symposium Digest of Technical Papers*, pp. 209–12, June 1994.
11. A. Ahumada, "Computational image-quality metrics: A review," *Society for Information Display Digest*, vol. SID-93 Digest, pp. 305–308, 1993.
12. M. P. Eckert and A. P. Bradley, "Perceptual quality metrics applied to still image compression," *Signal Processing*, pp. 177–200, Nov. 1998.
13. V. Algazi, N. Avadhanam, and Robert R. Estes, Jr., "Quality Measurement and use of Pre-processing in image compression," *Signal Processing*, pp. 215–229, Nov. 1998.
14. J. Lubin, "The use of psychophysical data and models in the analysis of display system performance," in *Digital Images and Human Vision* (A. Watson, ed.), Cambridge, Mass.: MIT Press, 1993.
15. J. Lubin, "A visual discrimination model for imaging system design and evaluation," in *Vision Models for Target Detection and Recognition* (E. Peli, ed.), Singapore: World Scientific, 1995.
16. D. Heeger, "Normalization of cell responses in cat visual cortex," *Visual Neuroscience*, vol. 9, pp. 181–197, 1992.
17. A. Bonds, "Role of inhibition in the specification of orientation selectivity of cells in the cat striate cortex," *Visual Neuroscience*, vol. 2, pp. 41–55, 1989.
18. A. Watson and J. Solomon, "Model of visual contrast gain control and pattern masking," *Journal of the Optical Society of America A (Optics, Image Science and Vision)*, vol. 14, pp. 2379–91, Sept. 1997.
19. J. Foley, "Human luminance pattern-vision mechanisms: masking experiments require a new model," *Journal of the Optical Society of America A (Optics, Image Science and Vision)*, vol. 11, pp. 1710–1719, June 1994.
20. P. Teo and D. Heeger, "A model of perceptual image fidelity," in *ICIP Proceedings, International Conference on Image Processing*, pp. vol.2 343–5, Oct. 1995.
21. A. Watson and J. Solomon, "Contrast gain control model fits masking data," *Investigative Ophthalmology and Visual Science*, vol. 36, no. 4, pp. Supplement, Abstract 2008, S438, 1995.
22. J. Solomon and A. Watson, "Spatial and spatial frequency spread of masking: Measurements and a contrast-gain-control model," *Perception*, vol. 24, pp. Supplement, 37, 1995.
23. S. Klein, T. Carney, L. Barghout-Stein, and C. Tyler, "Seven models of masking," in *Proceedings of SPIE, Human Vision and Electronic Imaging II*, pp. 13–24, 1997.
24. G. Legge and J.M.Foley, "Contrast masking in human vision," *Journal of the Optical Society of America A (Optics and Image Science)*, vol. 70, pp. 1458–1471, Dec. 1980.
25. A. Watson, "Probability summation over time," *Vision Research*, vol. 19, pp. 515–522, 1979.
26. N. Avadhanam and V. Algazi, "Image compression quality rating using anchored scales," in *Proceedings of SPIE, Very High Resolution and Quality Imaging Conference*, vol. 3307, 1998.
27. N. Avadhanam and V. Algazi, "Anchored subjective quality assessment scale for still image coding." *Signal Processing*, under review, 1998.
28. I. J. Group, "Independent JPEG group's free JPEG software." Home archive is <ftp.uu.net:/graphics/jpeg>.
29. J. Lu, V. Algazi, and Robert R. Estes, Jr., "A comparative study of wavelet image coders," *Optical Engineering*, vol. 35, pp. 2605–19, Sept. 1996.
30. V. Algazi and R.R. Estes, Jr., "Comparative performance of wavelet and JPEG coders at high quality," in *Proceedings of SPIE, Very High Resolution and Quality Imaging*, pp. 71–82, 1997.
31. M. Antonini, M. Barlaud, P. Mathieu, and I. Daubechies, "Image coding using wavelet transform," *IEEE Transactions on Image Processing*, vol. 1, pp. 205–220, Apr. 1992.
32. V. R. Algazi, G. E. Ford, and H. Chen, "Linear filtering of images based on properties of vision," *IEEE Transactions on Image Processing*, vol. 4, pp. 1460–1464, Oct. 1995.

33. T. A. Hentea and V. R. Algazi, "Perceptual models and the filtering of high-contrast achromatic images," *IEEE Trans. Sys., Man, and Cyber.*, vol. 14, no. 2, pp. 230–246, 1984.
34. A. Watson, "Efficiency of a model human image code," *Journal of the Optical Society of America A (Optics and Image Science)*, vol. 4, pp. 2401–17, Dec. 1987.
35. N. Jayant, J. Johnston, and R. Safranek, "Signal compression based on models of human perception," *Proceedings of the IEEE*, pp. 1385–1422, 1993.
36. D. Silverstein and J. Farrell, "The relationship between image fidelity and image quality," in *ICIP Proceedings, International Conference on Image Processing*, vol. 1, pp. 881–884, IEEE, 1996.
37. H. de ridder, "Psychophysical evaluation of image quality: from judgement to impression," in *Proceedings of SPIE, Human Vision and Electronic Imaging III*, 1998.